Published in final edited form as:
Chem Res Toxicol. 2006 November ; 19(11): 1506–1517. doi:10.1021/tx0601455.

Translesion Synthesis Past the C8- and N^2-Deoxyguanosine Adducts of the Dietary Mutagen 2-Amino-3-methylimidazo[4,5-*f*]quinoline in the *Nar*I Recognition Sequence by Prokaryotic DNA Polymerases

James S. Stover[†], **Goutam Chowdhury**[‡], **Hong Zang**[‡], **F. Peter Guengerich**[‡,§,⊥], and **Carmelo J. Rizzo**[*,†,§,⊥]
Departments of Chemistry and Biochemistry, Center in Molecular Toxicology, and Vanderbilt Institute of Chemical Biology, Vanderbilt University, Nashville, Tennessee 37235-1822

Abstract

2-Amino-3-methylimidazo[4,5-*f*]quinoline (IQ) is found in cooked meats and forms DNA adducts at the C8- and N^2-positions of dGuo after appropriate activation. IQ is a potent inducer of frameshift mutations in bacteria and is carcinogenic in laboratory animals. We have incorporated both IQ-adducts into the G_1-and G_3-positions of the *Nar*I recognition sequence (5′-$G_1G_2CG_3CC$-3′), which is a hotspot for arylamine modification. The in vitro replication of the oligonucleotides was examined with *Escherichia coli* pol I Klenow fragment exo$^-$, *E. coli* pol II exo$^-$, and *Sulfolobus solfataricus* P2 DNA polymerase IV (Dpo4), and the extension products were sequenced by tandem mass spectrometry. Replication of the C8-adduct at the G_3-position resulted in two-base deletions with all three polymerases, whereas error-free bypass and extension was observed at the G_1-position. The N^2-adduct was bypassed and extended by all three polymerases when positioned at the G_1-position, and the error-free product was observed. The N^2-adduct at the G_3-position was more blocking and was bypassed and extended only by Dpo4 to produce an error-free product. These results indicate that the replication of the IQ-adducts of dGuo is strongly influenced by the local sequence and the regioisomer of the adduct. These results also suggest a possible role for pol II and IV in the error-prone bypass of the C8-IQ-adduct leading to frameshift mutations in reiterated sequences, whereas noniterated sequences result in error-free bypass.

Introduction

Aromatic amines are an important class of chemical mutagens and carcinogens (1). Many simple carbocyclic arylamines such as 4-aminobiphenyl, 2-napthylamine, and benzidine are important industrial chemicals used in the dye industry; aminopyrene results from the in vivo reduction of nitropyrene, which is a combustion product of diesel fuel. Perhaps the most well-studied arylamines are 2-aminofluorene (AF)[1] and *N*-acetyl-2-amino-fluorene

[*]Corresponding author. Tel.: (615) 322-6100; fax: (615) 343-1234; c.j.rizzo@vanderbilt.edu.
[†]Department of Chemistry, Vanderbilt University.
[‡]Department of Biochemistry, Vanderbilt School of Medicine.
[§]Center in Molecular Toxicology, Vanderbilt University.
[⊥]Vanderbilt Institute of Chemical Biology.

Supporting Information Available: Figures and tables of CGE analysis of oligonucleotides, MALDI-TOF spectra of oligonucleotides, single-nucleotide incorporation of oligonucleotides, LC-ESI-MS/MS analysis, TIC and CID spectra, and CID fragmentation. This material is available free of charge via the Internet at http://pubs.acs.org.

(AAF), which were originally developed as pesticides but never used as intended because they were discovered to be animal carcinogens (2).

The browning of meats, poultry, and fish over high heat is a common culinary technique and a key flavoring step. Sugimura and co-workers demonstrated that this process produced compounds that were highly mutagenic in Ames *Salmonella typhimurium* assays (3). Over 20 mutagenic species that result from the pyrolysis of reducing sugars, amino acids, and proteins (Maillard reaction) have been structurally characterized (4, 5). These compounds were found to be heterocyclic aromatic amines (HCAs), and their distribution and concentration are dependent on the type of meat, cooking method, and temperature. In addition to the HCAs being highly mutagenic in bacteria, some were found to be carcinogenic in laboratory animals (6, 7). Given the widespread exposure of the HCAs through diet, they are likely contributors to human cancers (8). Consequently, there is significant interest in the biological processing of these DNA lesions.

All aromatic amines require prior metabolic activation before they can covalently modify DNA (9, 10). This involves oxidation of the aromatic amine to the hydroxylamine followed by esterification by *N*-acetyltransferase or sulfotransferase. The hydroxylamine esters undergo solvolysis to the corresponding nitrenium ion, which is the ultimate carcinogenic species. In general, aryl nitrenium ions react predominantly at the C8-position of dGuo. In some cases, a minor N^2-adduct has also been characterized (11, 12). Feeding studies with laboratory animals suggest that the minor N^2-adducts are more persistent due to less efficient repair and therefore may be more important to the carcinogenic properties of arylamines (1, 13, 14).

We have developed nonbiomimetic syntheses of the C8- and N^2-dGuo-adducts of 2-amino-3-methylimidazo[4,5-*f*]quinoline (IQ), one of the most mutagenic of the HCAs (Figure 1) (15–17). These lesions were site-specifically incorporated into oligonucleotides by solid-phase synthesis from the adducted phosphoramidite. Spectroscopic analysis of oligonucleotides containing the C8-adduct suggested that their conformation was highly dependent upon the specific sequence context (16). In a reiterated CG sequence, the IQ moiety adopted a base-displaced intercalated conformation but was largely groove-bound in a noniterated sequence (16, 18). Site-specific mutagenesis of the C8-AAF-adduct in the *Nar*I recognition sequence (5′-$G_1G_2CG_3$-CC-3′) resulted in a much higher frequency for two-base deletions when the adduct was incorporated at the G_3-position, which is part of a CG-dinucleotide repeat (19, 20). An intriguing hypothesis is that the greater proportion of the base-displaced inserted conformation in reiterated sequences leads to deletions, while the groove-bound conformation of noniterated sequences gives base-pair substitutions.

Fuchs and co-workers observed that treatment of bacteria with *N*-acetoxy-AAF resulted in a large number of two-base deletions in the *Nar*I recognition sequence (21). Reiterated sequences such as the CG–dinucleotide repeat found in the *Nar*I recognition sequence are prone to spontaneous and induced frameshift mutations; such mutations may be important contributors to human cancers (22). The *Nar*I sequence is regarded as a hotspot for arylamine modification and a prototype sequence for studing frameshift mutations (23). We have prepared oligonucleotides containing the *Nar*I recognition sequence in which the C8- or N^2-dGuo-adduct of IQ was site-specifically incorporated at the G_3- (reiterated) or G_1-positions (noniterated). The in vitro replication of these modified templates was examined

[1]Abbreviations: AF, 2-aminofluorene; AAF, 2-acetylaminofluorene; IQ, 2-amino-3-methylimidazo[4,5-*f*]quinoline; HCA, heterocyclic arylamine; Kf, *Escherichia coli* polymerase I, Klenow fragment (⁻ denotes exonuclease deficient); pol, polymerase; pol II⁻, *E. coli* DNA polymerase II (⁻ denotes exonuclease deficient); Dpo4, *Sulfolobus solfataricus* P2 DNA polymerase IV; UDG, uracil DNA glycosylase; ES, electrospray; TIC, total ion current; CID, collision-induced dissociation; BSA, bovine serum albumin; DTT, dithiothreitol; MALDI-TOF, matrix-assisted laser desorption/time-of-flight (MS).

by steady-state kinetics for single-nucleotide incorporation and full-length extension (standing start) assays using *Escherichia coli* DNA polymerase I Klenow fragment exo$^-$ (Kf$^-$), *E. coli* DNA polymerase II exo$^-$ (pol II$^-$), and *Sulfolobus solfataricus* P2 DNA polymerase IV (Dpo4). The sequences of the full-length extension products from pol II$^-$ and Dpo4 were determined using a robust LC-MS/MS strategy developed in our laboratories and provides mechanistic insight for the bypass of the IQ lesions. Our results suggest that the C8-IQ-adduct gives deletions when incorporated at the G_3-position and error-free bypass when incorporated at the G_1-position. In some cases, the N^2-adduct was more blocking but tended to give error-free products when bypassed by pol II$^-$ and Dpo4.

Experimental Procedures

Materials

Kf $^-$, pol II$^-$, and Dpo4 were expressed and purified as previously described (24, 25). Uracil DNA glycosylase (UDG) was purchased from Sigma Chemical Co. (St. Louis, MO). Piperidine was purchased form Aldrich and used as received. dNTP solutions (100 mM) were purchased from GE Healthcare (formerly Amersham Biosciences, Piscataway, NJ). [γ-^{32}P]ATP was purchased from NEN Life Sciences (Boston, MA). Unmodified oligonucleotides were purchased from Midland Certified Reagents (Midland, TX).

Labeling and Annealing of Oligonucleotides

The primer was 5′ end-labeled using T4 polynucleotide kinase with [γ-^{32}P]ATP and purified on a Biospin column (BioRad, Hercules, CA). Template and ^{32}P-labeled primer (1:1 molar ratio) were annealed in 50 mM Tris-HCl buffer (pH 7.8) by heating at 90 °C for 5 min and then slowly cooling to ≤30 °C.

Single-Nucleotide Incorporation Assays

^{32}P-labeled primers were annealed to either the unmodified or the modified (adducted) template, and extension reactions were then carried out in the presence of single dNTPs. All reactions were initiated by the addition of the dNTP (final dNTP concentration was 25, 50, and 100 μM) to preincubated enzyme/DNA mixtures giving a final reaction volume of 10 μL. The final concentrations for Dpo4 assays were 50 mM Tris-HCl (pH 7.8), 100 nM DNA duplex, 100 nM Dpo4, 1 mM dithiothreitol (DTT), 50 μg of bovine serum albumin (BSA) mL^{-1}, 50 mM NaCl, and 5 mM $MgCl_2$. The final concentrations for Kf$^-$ assays were 50 mM Tris-HCl (pH 7.8), 100 nM DNA duplex, 30–60 nM Kf $^-$, 1 mM DTT, 50 μg of BSA mL^{-1}, 50 mM NaCl, and 5 mM $MgCl_2$. The final concentrations for pol II$^-$ assays were 50 mM Tris-HCl (pH 7.8), 100 nM DNA duplex, 30–60 nM pol II$^-$, 1 mM DTT, 50 μg of BSA mL^{-1}, 50 mM NaCl, and 5 mM $MgCl_2$. Dpo4 reactions were run at 37 °C for 30 min, and Kf$^-$ and pol II$^-$ reactions were run at room temperature for 15 min. Reactions were quenched with 100 μL of 20 mM EDTA in 95% formamide (v/v) containing xylene cyanol and bromophenol blue dyes. Aliquots (4 μL) were separated by electrophoresis on a denaturing gel containing 8.0 M urea and 16% acrylamide (w/v) (from a 19:1 acrylamide/bisacrylamide solution, AccuGel, National Diagnostics, Atlanta, GA) with 80 mM Tris borate buffer (pH 7.8) containing 1 mM EDTA. The gel was exposed to a PhosphorImager screen (Imaging Screen K, Bio-Rad) overnight. The bands were visualized with a PhosphorImaging system (Bio-Rad, Molecular Imager FX) using the manufacturer's Quantity One software, version 4.3.0.

Full-Length Extension Assay with All Four dNTPs

A ^{32}P-labeled primer was annealed to either an unmodified or an adducted template and extended in the presence of all four dNTPs (100 μM each) at 37 °C for Dpo4 for 30 min or

to Kf$^-$ and pol II$^-$ at 25 °C for 15 min. Each reaction was initiated by adding the mixture of dNTPs to preincubated enzyme/DNA mixtures in a mixture of 50 mM Tris-HCl (pH 7.8), 100 nM DNA duplex, three varying concentrations of polymerases, 1 mM DTT, 50 μg of BSA mL^{-1}, 50 mM NaCl, and 5 mM $MgCl_2$, giving a final reaction volume of 10 μL. Reactions were quenched by the addition of 100 μL of 20 mM EDTA in 95% formamide (v/v) containing xylene cyanol and bromophenol blue dyes. Aliquots (4 μL) were separated by electrophoresis on a denaturing gel containing 8.0 M urea and 16% acrylamide (w/v) (from a 19:1 acrylamide/bisacrylamide solution, AccuGel, National Diagnostics, Atlanta, GA) with 80 mM Tris borate buffer, pH 7.8, containing 1 mM EDTA. Gels were exposed to a PhosphorImager screen (Imaging Screen K, Bio-Rad) overnight. The bands were visualized with a PhosphorImaging system (Bio-Rad, Molecular Imager FX) using the manufacturer's Quantity One software, version 4.3.0.

Steady-State Kinetics

A ^{32}P-labeled primer, annealed to either an unmodified or an adducted template, was extended in the presence of a single dNTP in the presence of a DNA polymerase (Dpo4, Kf$^-$, or pol II$^-$). Reaction times varied from 5 to 10 min (at 37 °C for Dpo4 and room temperature for Kf$^-$ and pol II$^-$). The molar ratio of primer–template/enzyme varied from 20:1 to 5:1 for modified oligonucleotides and up to 40:1 for unmodified oligonucleotides. Enzyme concentrations, dNTP concentrations, and reaction times were chosen so that the maximium product formation would be ~20% of the substrate concentration. All reactions (10 μL final volume) were run at eight dNTP concentrations (in duplicate) and quenched with 100 μL of 20 mM EDTA in 95% formamide (v/v) containing xylene cyanol and bromophenol blue dyes. Aliquots (4 μL) were separated by electrophoresis on denaturing gels containing 8.0 M urea and 16% acrylamide (w/ v) (from a 19:1 acrylamide/ bisacrylamide solution, AccuGel, National Diagnostics, Atlanta, GA) with 80 mM Tris borate buffer (pH 7.8) containing 1 mM EDTA. The gel was exposed to a PhosphorImager screen (Imaging Screen K, Bio-Rad) overnight. The bands were visualized with a PhosphorImaging system (Bio-Rad, Molecular Imager FX) using the manufacturer's Quantity One software, version 4.3.0. Graphs of rates versus dNTP concentration were fit using nonlinear regression (hyperbolic fits) in GraphPad Prism (version 4.0, GraphPad, San Diego, CA) for the estimation of k_{cat} and K_m values.

LC-MS/MS Analysis of Oligonucleotide Products from Dpo4, Kf$^-$, and pol II$^-$ Reactions

Dpo4, Kf$^-$, and pol II$^-$ reactions were performed for 6 h in 50 mM Tris-HCl (pH 7.8), 100–500 nM DNA duplex, 1 mM DTT, 50 μg of BSA mL^{-1}, 50 mM NaCl, and 5 mM $MgCl_2$ (200 μL total reaction mixture). The reactions were done with all four dNTPs at 1 mM each and polymerase concentrations of 100–500 nM Dpo4 and 60–200 nM Kf$^-$ and pol II$^-$, respectively. The reaction was terminated by extracting the dNTPs using a spin column (Bio-Spin 6, Bio-Rad). The concentrations of Tris-HCl, EDTA, and DTT were restored in the filtrate, and 20 units of UDG was added to the mixture. The reaction was allowed to incubate at 37 °C for 4 h. Piperidine (0.25 M) was added to the reaction mixture, which was then heated at 95 °C for 1 h followed by lyophilization to dryness. The residue was dissolved in 80 μL of H_2O for LC-MS/MS analysis.

MS was performed in the Vanderbilt facility on a DecaXP ion trap instrument (Thermofinnigan, San Jose, CA). The mixture was separated on a Jupiter microbore column (1.0 mm × 150 mm, 5 μm, Phenomenex, Torrance, CA). Buffer A contained 10 mM ammonium acetate (pH 6.8) and 2% CH_3CN (v/v). Buffer B contained 10 mM ammonium acetate (pH 6.8) and 98% CH_3CN (v/v). Using a flow rate of 0.1 mL min^{-1}, the gradient was 0–2 min, hold at 100% A; 2–20 min, linear program to 100% B; 20–30 min, hold at 100% B; 30–32 min, linear program to 100% A; and 32–40 min, hold at 100% A (for next

injection). Oligonucleotides eluted at retention times varying from 5 to 12 min. Samples were injected using an autosampler, with 10 μL withdrawn from the reaction mixture. Electrospray conditions were as follows: source voltage 3.4 kV, source current 8.5 μA, sheath gas flow-rate setting 28.2, auxiliary sweep gas flow-rate setting 4.3, capillary voltage 49 V, capillary temperature 230 °C, and tube lens voltage 67 V. MS/MS conditions were as follows: normalized collision energy 35%, activation *Q* 0.250, time 30 min, and one scan. Product ion spectra were acquired over the range *m*/*z* 300–2000. The abundant ions were selected for CID analysis. The calculations of the CID fragmentations of the candidate oligonucleotide sequence were done using the Mongo Oligo Mass Calculator (v. 2.6) from the Mass Spectrometry Group of Medicinal Chemistry at the University of Utah (http://library.med.utah.edu/masspec/).[2,3]

In the case of the sequence analysis Kf^{-}-catalyzed full-length extension, the initial analysis was equivocal, and subsequent LC-MS/MS was performed on a Waters Acquity UPLC system (Waters, Milford, MA) connected to a Finnigan LTQ mass spectrometer (ThermoElectron) using an Aquity UPLC BEH C18 column (1.7 μm, 1.0 mm × 100 mm). LC conditions were as follows: buffer A contained 10 mM $NH_4CH_3CO_2$ plus 2% CH_3CN (v/v) and buffer B contained 10 mM $NH_4CH_3CO_2$ plus 95% CH_3CN (v/v). The following gradient program was used with a flow rate of 150 μL min^{-1}: 0–3 min, linear gradient from 100% A to 97% A; 3–4.5 min, linear gradient to 80% A; 4.5–5 min, linear gradient 100% B; 5–5.5 min, hold at 100% B; 5.5–6.5 min, linear gradient to 100% A; and 6.5–9.5 min, hold at % A. The temperature of the column was maintained at 50 °C. Samples (10 μL) were infused with an auto-sampler. ES conditions were as follows: source voltage 4 kV, source current 100 μA, auxiliary gas flow-rate setting 20, sweep gas flow-rate setting 5, sheath gas flow setting 34, capillary voltage −49 V, capillary temperature 350 °C, and tube lens voltage −90 V. MS/MS conditions were as follows: normalized collision energy 35%, activation *Q* 0.250, and activation time 30 ms. Product ion spectra were acquired over the range *m*/*z* 345–2000 and analyzed as described previously.

Results

Oligonucleotide Synthesis

We have previously reported the site-specific incorporation of the IQ-modified dGuos into oligonucleotides using a manual coupling protocol (16). Using this method, the C8- and N^2-IQ-adducts of dGuo were incorporated into 27-mer oligonucleotides at the G_1- and G_3-positions of the *Nar*I recognition sequence (**1** and **2**, Figure 2). Oligonucleotides were >95% pure as judged by capillary gel electrophoresis and further characterized by MADLI-TOF mass spectrometry (Figures S1–S8 in the Supporting Information).[4]

[2]The nomenclature for the mass spectral CID fragments of the oligonucleotide is the same as proposed by McLuckey and coworkers (refs 28–31) and is shown below; −2 refers to the −2 charge state of the fragment.

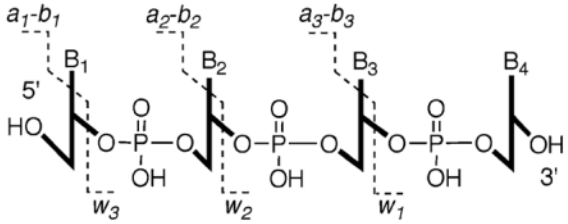

[3]The composition and theoretical CID spectrum of the extension products were calculated using the Oligo Composition Calculator (v. 1.2) and the Mongo Oligo Mass Calculator (v. 2.6), respectively. These web-based programs are maintained by the Department of Medicinal Chemistry, University of Utah and are available at http://library.med.utah.edu/masspec/.

[4]Figures and tables with an S preceding the number are found in the Supporting Information.

Translesion Synthesis by Kf $^-$

The Klenow fragment (Kf$^-$) inserted only dCTP opposite the C8- and N^2-IQ lesions. The insertion efficiency opposite the C8-IQ-adduct at the G_3-position (**1b**) was about 2300 times lower than for the unmodified template (**1a**) (Table 1). Incorporation of a second dCTP was also observed, suggesting a two-base slippage phenomenon (Figure S9). The insertion efficiency opposite the C8-adduct at the G_1-position (**2b**) was about 5-fold lower than at the G_3-position. There is a modest sequence effect for the incorporation of dCTP opposite the unmodified dGuo with the insertion opposite the G_1-position (**2a**) being nearly 2-fold more efficient than opposite G_3 (**1a**). The N^2-IQ-adduct at the G_3-position (**1c**) represented a significant block to replication by Kf$^-$, and no dNTP incorporation was observed. Incorporation opposite the N^2-adduct at the G_1-position (**2c**) was slightly less efficient than for the C8-adduct (**2b**).

In the presence of all four dNTPs (Figure 3A–F), the N^2-adduct at the G_1-position (**2c**) was extended most efficiently by Kf$^-$, giving a product that appeared to be one nucleotide short of full-length (Figure 3F). Interestingly, the C8-adduct at the G_3-position (**1b**), which appeared to give a two-base deletion in the single-nucleotide incorporation studies, was extended to give a 26-mer product, one base less than the expected full-length product (Figure 3B). The extension of **1b** stalled after the incorporation of one nucleotide (presumably dCTP); however, no intermediate that corresponded to incorporation of two nucleotides was observed, suggesting that insertion of the second dCTP may be rate-limiting for the two-base deletion mechanism. Extension of the C8-adduct at the G_1-position (**2b**) is completely inhibited after insertion of one nucleotide (Figure 3E). The N^2-IQ-adduct at the G_3-position was highly blocking (Figure 3C), while this adduct was bypassed and the primer extended when at the G_1-position (Figure 3F).

We further examined the extension of the C8-adduct at the G_3-position (**1b**) using a 20-mer primer with dCyd already positioned opposite the adduct. In single-nucleotide insertion assays, we observed that only dCTP was added to this primer, consistent with the extension of a two-base slippage template (Figure S10). When an additional dCyd was added to the primer (21-mer), we observed that only dGTP was incorporated, which is also consistent with the elongation of a two-base slipped conformation of the template (see Scheme 2 for the slippage mechanism).

To more fully understand the bypass mechanism of the C8-IQ-adducts by Kf$^-$ and other polymerases, we determined the nucleotide sequences of the extension products using an LC-MS/MS method recently reported by our laboratories (25–27). A dUrd was incorporated at position 17 of the primers and annealed to the modified templates (Scheme 1). After extension in the presence of all four dNTPs, the primer was hydrolyzed with uridine DNA glycosylase (UDG) followed by piperidine treatment to give a shorter oligonucleotide (≤10 nucleotides) that would be easier to analyze by MS. The extension products were then analyzed by LC-ESI-MS/MS. In general, we do not attempt to separate the extension products. Rather, they are coeluted, and all products are observed in the full-scan spectrum from the first sector. In this manner, the total ion current (TIC) spectrum provides the approximate relative distribution of extension products. Subsequent analysis of the collision-induced dissociation (CID) spectrum provides sequence information (28–31).

The LC-ESI/MS spectrum from the extension reaction of the C8-IQ-adduct at the G_3-position (**1b**) revealed that two products were formed with masses at *m*/*z* 842.5 and 946.7 (Figure 4A). These products were assigned as the [M – 3H] ions by the observation of the appropriate mass difference of the isotopic cluster (~0.3 Da). The mass difference between the products is 312.6 Da, indicating that they differ by a dAdo. Indeed, a composition calculator[3] gave three possibilities for *m*/*z* 2527.5 (±2), two of which were judged as

unlikely candidates given the sequences of the template and starting primer; the most likely composition consisted of two dCyds, one dTyd, four dGuos, one dAdo, and a phosphate ($pC_2T_1G_4A_1$). The sequence of 5′-pGGCCGAGT-3′ for the *m*/*z* 842.5 [M – 3H] product matched well with the predicted CID spectrum[3] and is the result of a two-base deletion opposite the C8-IQ-adduct followed by error-free extension (Figure 4B). The masses for the predicted and observed fragment ions from the CID spectrum are given in Table 2.[2,3] Analysis of the CID spectrum from the second product (*m*/*z* = 946.7) indicated that its sequence was 5′-pGGCCGAGTA-3′ and arises from a two-base deletion opposite the IQ-adduct followed by error-free extension and a blunt end addition of dATP (Figure 4C). The sequences could be differentiated by the presence of w_1 and w_2 fragment ions at *m*/*z* 321.1 and 650.2 for the *m*/*z* 842.5 product, which correspond to the pT-3′ and pGT-3′ ions.[3] The *m*/*z* 946.7 product possessed a w_2 ion at *m*/*z* 634.1, which corresponds to a p-TA-3′ fragment. The a-B ion series, which sequences from the 5′ end, were very similar for both products. The peaks in the TIC spectrum at *m*/*z* 1264.0 and 1420.6 represent the [M – 2H] charge state of these products. The ratio of the extension products (842.5 + 1264.0/946.8 + 1420.6) was ~2:1.

One major product was identified from the Kf^- extension of the N^2-IQ-adduct at the G_1-position (**2c**) with *m*/*z* of 1152.8 (Figure 5A). The composition of this product was calculated to be $pC_3T_1G_5A_2$ for an [M – 3H] ion, and the mass at *m*/*z* 864.8 represents the [M– 4H] ion. Analysis of the CID spectrum (Figure 5B) indicated that its sequence is 5′-pGGCGCCGAGTA-3′ and corresponds to an error-free extension product with a blunt end addition of dATP. A nearly complete set of a-B and w ions provide strong evidence for this sequence and are given in Table 3. The identity of the minor product of *m*/*z* 1011.3 could not be determined. A summary of the KF^- extension and product analysis is given in Table 4.

Translesion Synthesis by *E. coli* pol II$^-$

Pol II$^-$ favored insertion of dGTP over dCTP opposite the C8-IQ-adduct at the G_3-position (**1b**) with catalytic efficiencies (k_{cat}/K_m) significantly lower than the insertion of dCTP opposite an unmodified dGuo (Figure S11 and Table 4). The efficiency for dGTP insertion opposite the C8-IQ-adduct in oligonucleotide **1b** was only 2-fold lower than misincorporation opposite an unmodified template. In addition to a simple misinsertion, the incorporation of dGTP is consistent with a one-base slippage, while incorporation of dCTP is consistent with a two-base slippage or error-free bypass. In the presence of all four dNTPs, pol II$^-$ extended **1b** to give a full-length extension product plus a minor product that was one base shorter (Figure 3H). When the C8-IQ-adduct was incorporated into the noniterated G_1-position (**2b**), we observed only incorporation of dCTP (Table 5); the catalytic efficiency of dCTP incorporation was 2600 times worse than for the unmodified template. In the presence of all four dNTPs, the primer was efficiently extended past the C8-adduct of **2b** to give a 27-mer (full-length) and 26-mer product (Figure 3K).

LC-ESI/MS analysis of the pol II$^-$ extension of **1b** showed that two products were produced with *m*/*z* of 944.1 and 1053.7 in a 1.2:1 ratio as judged by the TIC spectrum (Figure S13). Assignment of these products as the [M – 3H] ions gave a mass difference of 327 Da, indicating that they differ in composition by a dGuo. The most likely oligonucleotide composition for *m*/*z* 2832.2 (±2) was calculated to be $pC_2T_2G_4A_1$. The sequence of 5′-pGGCCGAGTT for the *m*/*z* 944.1 product matched well with the predicted CID spectrum (Figure S14) and is the result of a two-base deletion opposite the C8-IQ-adduct followed by error-free extension and a blunt end addition of a dThd. The predicted fragments with the observed masses from the CID spectrum are given in Table S1 of the Supporting Information. Analysis of the CID spectrum of the second product from the extension of oligonucleotide **1b** (*m*/*z* = 1053.73, Figure S16) indicated that its sequence was 5′-pGGGCCGAGTT-3′ and arises from a one-base deletion opposite the IQ-adduct and

subsequent error-free extension. The addition of dATP is the more common outcome of a noninstructive blunt end addition (32). The unusual blunt end addition of dThd, which was identified by the presence of a w_2 fragment ion at *m*/*z* 625.2 (pTT-3′) in the CID spectrum (Figures S14 and S16), probably arises from a misalignment at the end of the template and primer and subsequent insertion opposite the 5′-terminal dAdo.

The mechanism for one- and two-base deletions is shown in Scheme 2. The relative efficiencies for single-nucleotide insertion of dCTP opposite the C8-adduct of **1b** by pol II$^-$ is 43-fold lower than for dGTP. This suggests that the subsequent extension from the initial insertion of dCTP leading to the two-base deletion product is significantly more favorable than the extension from the initial insertion of dGTP leading to the one-base deletion product.

A single product from the pol II$^-$ extension of the C8-IQ-adduct at the noniterated G_1-position (**2b**) was observed by LC-MS with an *m*/*z* of 1152.8 (Figure S19), which was assigned as an [M – 3H] ion and predicted to be composed of $pC_3T_1G_5A_2$. Analysis of the CID spectrum (Figure S20 and Table S3) indicated that the product was an error-free bypass and extension of the **2b** followed by a blunt end addition of dAdo (5′-pGGCGCCGAGTA-3′).

The catalytic efficiency for insertion of dCTP and dGTP opposite the N^2-IQ-adduct at the G_3-position (**1c**) by pol II$^-$ was poor, and further extension was blocked (Table 5 and Figure 3I). Pol II$^-$ inserted only dCTP opposite the N^2-adduct at the noniterated G_1-position (**2c**), although the catalytic efficiency was significantly lower than for the unadducted oligonucleotide. Pol II$^-$ was able to extend the primer past the N^2-lesion of **2c** to give a full-length product (Figure 3L). LC-MS analysis of the extension reaction showed that a single product was produced with an *m*/*z* of 1048.7 (Figure S22). The CID spectrum (Figure S23 and Table S4) was a good match to the predicted fragmentation for the error-free bypass and extension product (5′-pGGCGCCGAGT-3′).

In summary, pol II$^-$ replication resulted in one- and two-base deletions when the C8-IQ-adduct was placed at the G_3-dinucleotide repeat position of the *Nar*I recognition sequence (**1b**) but error-free bypass and extension when the adduct was at the noniterated G_1-position (Table 6). Pol II$^-$ favored incorporation of dCTP over dGTP opposite the regioisomeric N^2-IQ-adduct when placed at the G_3-position (**1c**) but was unable to extend either of these initial insertion products. Pol II$^-$ replication of the N^2-adduct at the G_1-position (**2c**) resulted in an error-free extension product.

Translesion Synthesis by Dpo4

Dpo4 favors insertion of dCTP opposite the C8-IQ lesion at both the G_1- and the G_3-positions with catalytic efficiencies about 450 times lower than insertion opposite an unmodified template (Table 7). At higher dCTP concentrations, a less efficient insertion of a second dCTP was observed with **1b**, which is consistent with a two-base deletion. dTTP was also inserted opposite the G_3-modified oligonucleotide **1b** with a misincorporation frequency of 0.13 (cf. dCTP). Extension past the modified base was observed at both positions for the C8-adduct, although the major product from the G_3-modified template (**1b**) appears to be one and two bases shorter than the expected full-length 27-mer (Figure 3N). The catalytic efficiency for dCTP insertion opposite the N^2-adduct at the G_3-position (**1c**) was about 1 order of magnitude lower than for the C8-adduct (**1b**) and ~65% lower than the N^2-adduct at the G_1-position (**2c**). Dpo4 also inserted dGTP opposite the N^2-adduct at the G_3-position (**1c**) with a misincorporation frequency of 75%. Insertion of all four nucleotides was observed opposite the N^2-adduct at the G_1-position (**2c**) with a misincorporation frequency ranging from 9 to 46% (Figure S25) (33). Dpo4 was able to extend the N^2-adduct

(**1c** and **2c**) to give full-length products in both sequences (Figure 3O,R). In contrast to pol II⁻, the efficiency for dCTP insertion opposite the unmodified templates **1a** and **2a** by Dpo4 showed a modest sequence effect with the insertion being about 2-fold more efficient at the reiterated G_3-position (**1a**).

LC-MS/MS analysis was used to identify a single unique product (*m*/*z* 1043.6) from the extension of **1b** with Dpo4 (Figure S27). This product was identified as an [M – 3H] ion with a composition of pC_4G_5A. The sequence of this extension product (5′-pGGCCCGCGAG-3′) was determined by LC-MS/ MS after UDG hydrolysis and was unusual in that it contained a number of mismatches downstream from the adduct (Figure S28 and Table S5). Significant to this study, the extension product is consistent with an initial two-base deletion. A tentative mechanism for the bypass and extension of **1b** to give the observed product is shown in Scheme 3 and involves a number of template–primer realignments, which may reflect the low processivity of Dpo4. The Dpo4 extension product from **2b** had a *m*/*z* value of 1048.5, which corresponds to the error-free bypass and extension product (5′-pGGCGCCGAGT-3′); the sequence of this product was confirmed by analysis of its CID spectrum (Figure S32 and Table S6).

Replication of both N^2-IQ-modified templates (**1c** and **2c**) with Dpo4 resulted in single products with an *m*/*z* 1153.1 and 1048.8, respectively. These products have the same nominal masses expected for the error-free bypass and extension products with and without a blunt end addition of dATP, which were observed previously. Analysis of the CID spectra indicated that these products were indeed derived from error-free replication of the N^2-adduct.

Table 8 summarizes our results for the translesion synthesis of the IQ-modified oligonucleotides by Dpo4. In all cases examined, extension was observed only after the initial insertion of dCTP opposite the IQ-adducts. Replication of the C8-IQ-adduct at the G_1-position (**2b**) and the *N*2-adduct at the G_1- and G_3-positions resulted in error-free extension products (**1c** and **2b**). In the case of the C8-adduct at the reiterated G_3-position (**1b**), we observed an initial two-base deletion and subsequent error-prone extension.

Discussion

IQ is among the most mutagenic of the HCAs and is significantly more mutagenic than benzo[*a*]pyrene and aflatoxin B_1 in Ames assays (3). Detailed studies on the biological processing of IQ- and other HCA-adducts using site-specifically adducted oligonucleotides have been limited due to a lack of synthetic accessibility (34, 35). A wealth of studies have been reported on the C8-dGuo-adducts of AF and AAF, including in vivo and in vitro replication studies, repair studies, and structural analyses (2, 36). Similar studies on the minor N^2-dGuo-adduct of AAF are emerging (37–39).

The *Nar*I recognition sequence (5-$G_1G_2CG_3$CC-3′) is considered a hot spot for arylamine modification, and the AF- and AAF-adducts have been studied extensively in this sequence (21, 40). Although structurally similar, AF and AAF elicit significantly different biological responses. For example, the C8-dGuo-adduct of AF is bypassed by the *E. coli* pol III holoenzyme, although the efficiency of the bypass is dependent on the sequence (20, 41). Pol III bypassed the C8-AF-adduct at the G_3-position of the *Nar*I recognition sequence with noticeably lower efficiency than modification of the G_1- or G_2-positions (20). In contrast, DNA synthesis was arrested when pol III encountered the C8-AAF-adduct at all three positions. These results are in accord with the observation that the mutagenicity of AF is SOS independent while AAF requires an SOS-dependent mechanism (42). Additionally, AF and AAF elicit different types of mutations. AAF gives largely one-base deletions in runs of

dGuo's and two-base deletions in CG-dinucleotide repeat sequences (19, 21, 43–45). The C8-AF-adduct induces base-pair substitutions of which G → T transversions are the most prominent. Site-specific mutagenesis of the C8-AAF-adduct at all three positions of the *Nar*I recognition sequence in SOS-induced *E. coli* revealed that the majority of the two-base deletions occurred when the G_3-position was modified (46). The C8-AF-adduct did not produce any deletions independent of the sequence context.

Differences in the processing of the C8-AF- and AAF-adducts by DNA polymerases have been attributed to distinct conformations (20, 47, 48). Solution structures of oligonucleotides containing site-specific C8-AF, AAF, and other simple aromatic amine derivatives have been determined by a combination of NMR and constrained molecular dynamics calculations (36, 49–62). These studies have indicated that the C8-AAF-adduct favors a base-displaced intercalated conformation and is significantly more distorted than the C8-AF-adduct, which is predominately groove-bound. The structures of the C8-dGuo-adduct of the heterocyclic amine 2-amino-1-methyl-6-phenylimidazo[4,5-*b*]-pyridine (PhIP) in a noniterated sequence as well as the C8-IQ-adduct at the G_3-position of the *Nar*I recognition sequence have been determined (18, 63); these C8-HCAs have a strong preference for the base-displaced intercalated conformation, similar to AAF. Conformational preferences due to adduct structure or local sequence effects can lead to different interactions within the polymerase active site and consequently lead to different mutagenic outcomes. Crystallographic analyses of AF- and AAF-modified oligonucleotides bound to high-fidelity DNA polymerases have provided a more detailed structural basis for the mechanism of bypass and inhibition by these adducts (64, 65).

IQ is a potent inducer of one- and two-base frameshift deletions in reiterated sequences. The mutagenicity of IQ was reported to be SOS independent (66). Thus, the interaction between DNA polymerases and IQ-adducts may share properties with both AF and AAF. It should be noted that the mutagenicity of the closely related 2-amino-3,8-dimethylimidazo[4,5-*f*]-quinoxaline (MeIQx) was reported to be enhanced 6-fold upon SOS induction (67). Replication studies of the IQ-adducts using site-specifically modified oligonucleotides have not been evaluated to date. Using synthetic approaches previously developed in our labs, the C8- and N^2-dGuo-adducts of IQ were site-specifically incorporated at the G_1- and G_3-positions of the *Nar*I recognition sequence. These two positions were chosen because we have insight into the conformation of the C8-IQ-adduct in these sequences (16, 18).

E. coli DNA polymerase I (Kf^-) is readily available and often used to evaluate the effect of DNA lesions on the mechanism and fidelity of DNA replication. The bypass of the C8-dGuo-adducts of AF and AAF has been extensively studied with Kf. Translesion synthesis and extension of the C8-AF-adduct was reported at all three dGuo positions of the *Nar*I sequence with Kf^-, although there were significant pauses at the adduct site and one base prior. Interestingly, exonuclease proficient Kf (Kf^+) was not able to extend pass the C8-AF-adduct when it was at the G_3-position (20). Bacteriophage pol $T7^-$ also bypassed the C8-AF-adduct at the G_1- and G_2-positions, but polymerization was blocked one base prior, one base after, and at the adduct site when incorporated at the G_3-position (68).

The C8-AAF-adduct represents a strong block to replication; however, when the lesion is bypassed, insertion of dCTP was favored, although the efficiency of incorporation can be as much as 10^6 lower than the unmodified oligonucleotide (68, 69). Gill and Romano examined the C8-AAF-adduct at the G_3-position of the *Nar*I recognition sequence and found that when Kf^- bypassed the lesion, a two-base deletion resulted (70). The bypass and extension of the C8-IQ-adduct at the G_3-position by Kf^- resulted in a two-base deletion and paralleled the results of Gill and Romano for the C8-AAF-adduct in the same local sequence context.

Extension of an N^2-AAF-adduct by Kf in a noniterated sequence has been reported to insert all four dNTPs with varying efficiencies, although further extension was most efficient when dAdo was opposite the N^2-adduct (37). We observed that Kf$^-$ inserted only dCTP opposite the N^2-IQ-adduct at the noniterated G_1-position and that further extension was efficient and error-free. No dNTP incorporation was observed opposite the N^2-IQ-adduct at the G_3-position.

The three SOS-inducible DNA polymerases in *E. coli*—pol II, pol IV, and pol V—can all be involved in the replication of damaged DNA. Using in vivo and in vitro methods, Fuchs observed that pol II and IV were responsible for error-prone bypass of the C8-AAF-adduct and that pol II was specifically responsible for two-base deletions when incorporated at the G_3-position of the *Nar*I recognition sequence (71–73); on the other hand, error-free bypass of AAF-adducted DNA was observed with pol V. In vitro extension of the C8-AAF-adduct at the G_3-position of the *Nar*I sequence with pol II resulted in one- and two-base deletions (73).

We observed a striking sequence dependence for the in vitro bypass of the C8-adduct by pol II$^-$. One- and two-base deletions were observed with equal frequency for the translesion synthesis across the C8-IQ-adduct at the GC-repeat portion of the *Nar*I sequence (**1b**), but error-free bypass and extension were observed at the noniterated G_1-position (**2b**). The observation that replication of oligonucleotide **1b** with pol II$^-$ results in one- and two-base deletions parallels the results of Becherel and Fuchs with the C8-AAF-adduct in the same local sequence context (73).

Pol II$^-$ was able to insert dCTP or dGTP opposite the N^2-adduct at the G_3-position, but further extension was completely inhibited, while this adduct led to error-free bypass and extension when incorporated at the noniterated G_1-position (**2c**). If bypass of IQ-adducts by pol II is the in vivo mechanism for two-base deletions in bacteria as in the case of the AAF-adducts, our studies suggest that the N^2-IQ-adduct does not play a significant role in this particular mutagenic outcome. This result is in contrast to our recent in vitro analysis with human Y-family polymerases (74). In this work, we found that both the C8- and the N^2-regioisomer represented significant blocks to replication with human pol δ, ι, and κ but were bypassed and extended by hpol η. Interestingly, bypass and extension of the C8-adduct resulted in error-free products, while the N^2-adduct led to a two-base deletion when positioned at the reitertaed G_3-position (**1c**). These observations implicate the minor N^2-IQ-adduct in repeat sequences as the important premutagenic lesion in mammals.

Dpo4 is an archaeal *Din*B homologue related to *E. coli* pol IV and eukaryotic pol κ, although it possesses lesion bypass properties similar to pol η (*RAD30*) (75, 76). Crystallographic analyses of modified oligonucleotides bound to Dpo4 have been reported and provide valuable insight into the mechanism of lesion bypass (25, 26, 77–80). Dpo4 gives rise to one-base deletions when it replicates through the 1, N^2-etheno-dGuo and the tetrahydrofuran model lesion for an abasic site (25, 78); these deletions arose from significantly different geometries of the bound templates. Previous studies showed that Dpo4 exclusively inserted dCTP opposite a C8-AAF in a noniterated sequence (75). The in vitro replication of the C8-AAF and AF-adducts have been examined in a noniterated sequence with *E. coli* pol IV (81). The bypass was inefficient for both adducts, and extension was blocked at the adduct site and one base prior. When the primer was extended, one- and two-base deletions were the major miscoding event accompanied by misinsertion of dATP, dGTP, and dCTP. Significant error-free bypass and extension were also observed.

We found that replication of the C8-IQ-adduct at the G_3-position of the *Nar*I sequence by Dpo4 also resulted in a two-base deletion. Further extension past the adduct was inefficient

and error-prone. Pause sites were observed at the adduct site and to a lesser extent one base after. Further analysis of the extension reaction revealed numerous minor pauses between the adduct site and the final product (Figure 4E). The low processivity of Dpo4 may contribute to the inefficient and error-prone extension of **1b**. Interestingly, Dpo4 was able to bypass and extend the other oligonucleotides (**2b**, **1c**, and **2c**) in an error-free manner; however, the efficiency of the extension appeared to vary depending on the regioisomer and sequence context. The extension of the C8-adducts (**1b** and **2b**) appeared to be more efficient than for the N^2-adducts (**1c** and **2c**).

Replication of the C8-IQ-adduct at the reiterated G_3-position of the *Nar*I sequence (**1b)** resulted in two-base deletions with all three polymerases studied; additionally, an equal proportion of a one-base deletion product was observed with pol II$^-$. Structural studies of the C8-IQ-adduct in this local sequence context (in the absence of polymerase) showed that it exists in the base-displaced intercalated conformation with a *syn*-glycosidic geometry (18). Insertion of dCTP requires that the modified dGuo be in the *anti*-geometry. Modeling studies of the C8-AAF-adduct in the active site of Dpo4 suggest that hydrogen-bonding of dCTP to the *anti*-conformation can be accommodated with minimal perturbation (82). The current model for two-base slippage involves an error-free insertion of dCTP opposite the C8-modified dGuo followed by a conformational reorganization to the slippage intermediate (23). DNA replication is inhibited or significantly slowed by damaged DNA bases, and this slowed progression of the replication fork may allow for a conformational exchange after insertion of dCTP across from the adduct. The active sites of lesion bypass polymerases are often spacious and may be able to accommodate the extra helical loop of the slipped conformation. The active site should be equally capable of accommodating the one-base slippage intermediate as well.

The mechanism for the one-base deletion may involve direct insertion of dGTP opposite the dCyd that is 5′ to the extrahelical, modified base (as shown in Scheme 2). Alternatively, the deletion may involve a misinsertion of dGTP opposite the modified base followed by slippage and extension (83). This misinsertion may utilize a Hoogsteen interaction with the incoming dGTP with the *syn*-conformation of the C8-modified dGuo. Crystallographic and kinetic studies suggest that that nascent Hoogsteen pairing between template and dNTP may play an important role for error-free translesion synthesis by pol *ι* (84–86).

Dpo4 inserted only dCTP opposite the C8-IQ-adduct at the noniterated G_1-position. Preliminary structural analysis indicated that the C8-adduct adopts a predominately groove-bound conformation in noniterated sequences. A groove-bound conformation for the C8-modified dGuo would allow for Watson–Crick pairing between modified base and incoming dCTP. The preference for the IQ moiety to remain groove-bound in noniterated sequences and not undergo a conformational exchange to a slippage intermediate during the elongation of the primer may play a role in such noniterated sequences giving base-pair substitution rather than frameshift mutations.

Forward mutation analysis in *E. coli* treated with IQ using the yeast *URA3* reporter gene showed that the predominant base-pair substitution mutation was a G → A transition, followed by G → T and G → C transversions (87). In single-nucleotide insertion experiments, we observed misinsertions opposite the modified base with pol II and Dpo4; however, most of these initial misinsertions opposite the IQ-adduct were not extended. It is possible the initial misinsertions are further extended at very low efficiency and below the detection limits of our MS analysis. Dpo4 is the most error prone of the polymerases examined for the IQ-adducts, and this result suggests that pol IV may be the source for the base-pair substitution mutations in bacteria. Of note, Dpo4 gave extension products for the C8-adduct at the G_1-position (**1c**) and the N^2-adduct at the G_3-positions (**2b**), whereas pol

II$^-$ and Kf$^-$ did not. It is likely that cells use multiple DNA polymerases to replicate damaged DNA, and our observations may indicate a specialized role for pol IV in the bypass of a specific regioisomer of the IQ-adduct as well as in specific sequence contexts.

Differences in the bypass of the C8-AAF-adducts in the *Nar*I sequence have been attributed to different sequence-dependent, local conformations of the modified base. The different conformations of the C8-IQ-adduct at the G_1- (groove-bound) and G_3-positions (intercalated) correlate to specific polymerase bypass products (deletions vs error-free bypass) and fit this hypothesis. The dramatic difference in the ability of *E. coli* pol II$^-$ to bypass the N^2-adducts depending on the local sequence may be indicative of sequence dependent, conformational preferences for this regiosiomer as well.

In summary, we have examined the in vitro bypass and extension of the C8- and N^2-dGuo-adducts of the dietary mutagen IQ at the G_3- and G_1-positions of the *Nar*I recognition sequence. Our results suggest a role of pol II and perhaps pol IV in the bypass of C8-IQ-adducts leading to two-base deletions. The SOS-inducible polymerases are expressed in low constitutive levels and are believed to be involved in the rescue of stalled replication forks (88, 89). These phenomena may provide a partial explanation for IQ mutagenesis being SOS independent. In vitro analysis of the IQ-adducts with the other *E. coli* polymerases (pol III, IV, and V) as well as exonuclease proficient polymerases may provide further insight into the mechanism of bypass.

Supplementary Material

Refer to Web version on PubMed Central for supplementary material.

Acknowledgments

This work was supported in part by National Institutes of Health research Grants R01 ES01375 (F.P.G.) and P30 ES00267 (C.J.R. and F.P.G.). J.S.S. was supported by T32 ES007028. H.Z. and G.C. were supported by a Merck Research Research Fellowship. We thank L. L. Furge for preparing Kf$^-$ and pol II$^-$ and J.-Y. Choi and K. C. Angel for preparing Dpo4. We also thank L. Manier for technical assistance with the MS experiments.

References

1. Beland FA, Kadlubar FF. Formation and persistence of arylamine DNA adducts in vivo. Environ Health Perspect. 1985; 62:19–30. [PubMed: 4085422]
2. Heflich RH, Neft RE. Genetic toxicity of 2-acetylaminofluorene, 2-aminofluorene, and some of their metabolites and model metabolites. Mutat Res. 1994; 318:73–174. [PubMed: 7521935]
3. Sugimura T. Overview of carcinogenic heterocyclic amines. Mutat Res. 1997; 376:211–219. [PubMed: 9202758]
4. Jagerstad M, Skog K, Arvidsson P, Solyakov A. Chemistry, formation, and occurrence of genotoxic heterocyclic amines identified in model systems and cooked foods. Z Lebensm-Unters-Forsch. 1998; 207:419–427.
5. Skog KI, Johansson MA, Jagerstad MI. Carcinogenic heterocyclic amines in model systems and cooked foods: A review on formation, occurrence, and intake. Food Chem Toxicol. 1998; 36:879–896. [PubMed: 9737435]
6. Schut HA, Snyderwine EG. DNA adducts of heterocyclic amine food mutagens: Implications for mutagenesis and carcinogenesis. Carcinogenesis. 1999; 20:353–368. [PubMed: 10190547]
7. Turesky RJ. Heterocyclic aromatic amine metabolism, DNA adduct formation, mutagenesis, and carcinogenesis. Drug Metab Rev. 2002; 34:625–650. [PubMed: 12214671]
8. Sugimura T. Nutrition and dietary carcinogens. Carcinogenesis. 2000; 21:387–395. [PubMed: 10688859]

9. Kim D, Guengerich FP. Cytochrome P450 activation of arylamines and heterocyclic amines. Annu Rev Pharmacol Toxicol. 2005; 45:27–49. [PubMed: 15822170]
10. Guengerich FP. *N*-Hydroxylarylamines. Drug Metab Rev. 2002; 34:607–623. [PubMed: 12214670]
11. Turesky RJ, Markovic J. DNA adduct formation of the food carcinogen 2-amino-3-methylimidazo[4,5-*f*]quinoline at the C8 and N2 atoms of guanine. Chem Res Toxicol. 1994; 7:752–761. [PubMed: 7696529]
12. Turesky RJ, Rossi SC, Welti DH, Lay JO, Kadlubar FF. Characterization of DNA adducts formed in vitro by reaction of *N*-hydroxy-2-amino-3-methylimidazo[4,5-*f*]quinoline and *N*-hydroxy-2-amino-3, 8-dimethylimidazo[4,5-*f*]quinoxaline at the C8 and N2 atoms of guanine. Chem Res Toxicol. 1992; 5:479–490. [PubMed: 1391614]
13. Turesky RJ, Box RM, Markovic J, Gremaud E, Snyderwine EG. Formation and persistance of DNA adducts of 2-amino-3-methylimidazo[4,5-*f*]quinoline in the rat and nonhuman primates. Mutat Res. 1997; 376:235–241. [PubMed: 9202760]
14. Seeberg E, Fuchs RP. Acetylaminofluorene bound to different guanines of the sequence -GGCGCC- is excised with different efficiencies by the UvrABC excision nuclease in a pattern not correlated to the potency of mutation induction. Proc Natl Acad Sci USA. 1990; 87:191–194. [PubMed: 2296578]
15. Stover JS, Rizzo CJ. Synthesis of the N^2-deoxyguanosine adduct of the potent dietary mutagen IQ. Org Lett. 2004; 6:4985–4988. [PubMed: 15606116]
16. Elmquist CE, Stover JS, Wang Z, Rizzo CJ. Site-specific synthesis and properties of oligonucleotides containing C8-deoxyguanosine adducts of the dietary mutagen IQ. J Am Chem Soc. 2004; 126:11189–11201. [PubMed: 15355100]
17. Wang Z, Rizzo CJ. Synthesis of the C8-deoxyguanosine adduct of the food mutagen IQ. Org Lett. 2000; 3:565–568. [PubMed: 11178826]
18. Wang F, De Muro NE, Elmquist CE, Stover JS, Rizzo CJ, Stone MP. Base-displaced intercalated structure of the food mutagen 2-amino-3-methylimidazo[4,5-*f*]quinoline (IQ) in the recognition sequence of the *Nar*I restriction enzyme, a hotspot for −2 bp deletions. J Am Chem Soc. 2006; 128:10085–10095. [PubMed: 16881637]
19. Tan X, Suzuki N, Grollman AP, Shibutani S. Mutagenic events in *Escherichia coli* and mammalian cells generated in response to acetylaminofluorene-derived DNA adducts positioned in the *Nar*I restriction enzyme site. Biochemistry. 2002; 41:14255–14262. [PubMed: 12450390]
20. Belguise-Valladier P, Fuchs RPP. *N*-2-Aminofluorene and *N*-2-acetylaminofluorene-adducts: The local sequence context of the adduct and its chemical structure determines its replication properties. J Mol Biol. 1995; 249:903–913. [PubMed: 7791216]
21. Fuchs RP, Schwartz N, Daune MP. Hot spots of frameshift mutations induced by the ultimate carcinogen *N*-acetoxy-*N*-2-acetylaminofluorene. Nature. 1981; 294:657–659. [PubMed: 7031481]
22. Duval A, Hamelin R. Mutations at coding repeat sequences in mismatch repair-deficient human cancers. Toward a new concept of target genes for instability. Cancer Res. 2002; 62:2447–2454. [PubMed: 11980631]
23. Hoffmann GR, Fuchs RPP. Mechanisms of frameshift mutations: Insight from aromatic amines. Chem Res Toxicol. 1997; 10:347–359. [PubMed: 9114969]
24. Lowe LG, Guengerich FP. Steady-state and pre-steady-state kinetic analysis of dNTP insertion opposite 8-oxo-7, 8-dihy-droguanine by *Escherichia coli* polymerases I exo^- and II exo^-. Biochemistry. 1996; 35:9840–9849. [PubMed: 8703958]
25. Zang H, Goodenough AK, Choi JY, Irimia A, Loukachevitch LV, Kozekov ID, Angel KC, Rizzo CJ, Egli M, Guengerich FP. DNA adduct bypass polymerization by *Sulfolobus solfataricus* DNA polymerase Dpo4: Analysis and crystal structures of multiple base-pair substitution and frameshift products with the adduct 1,N^2-ethenoguanine. J Biol Chem. 2005; 280:29750–9764. [PubMed: 15965231]
26. Zang H, Irimia A, Choi JY, Angel KC, Loukachevitch LV, Egli M, Guengerich FP. Efficient and high fidelity incorporation of dCTP opposite 7,8-dihydro-8-oxodeoxyguanosine by *Sulfolobus solfataricus* DNA polymerase Dpo4. J Biol Chem. 2006; 281:2358–2372. [PubMed: 16306039]

27. Choi JY, Zang H, Angel KC, Kozekov ID, Goodenough AK, Rizzo C, Guengerich FP. Translesion synthesis across 1,N^2-ethenogunaine by human DNA polymerases. Chem Res Toxicol. 2006; 19:879–886. [PubMed: 16780368]
28. Ni J, Pomerantz SC, Rozenski J, Zhang Y, McCloskey JA. Interpretation of oligonucleotide mass spectra for determination of sequence using electrospray ionization and tandem mass spectrometry. Anal Chem. 1996; 68:1989–1999. [PubMed: 9027217]
29. McLuckey SA, Van Berker GJ, Glish GL. Tandem mass spectrometry of small, multiply charged oligonucleotides. J Am Soc Mass Spectrom. 1992; 3:60–70.
30. McLuckey SA, Habibi-Goudarzi S. Decompositions of multiply charged oligonucleotide anions. J Am Chem Soc. 1993; 115:12085–12095.
31. McLuckey SA, Vaidyanathan G, Habibi-Goudarzi S. Charged versus neutral nucleobase loss from multiply charged oligonucleotide anions. J Mass Spectrom. 1995; 30:1222–1229.
32. Clark JM, Joyce CM, Beardsley GP. Novel-blunt end addition reactions catalyzed by DNA polymerase I of *Escherichia coli*. J Mol Biol. 1987; 198:123–127. [PubMed: 3323527]
33. Perlow-Poehnelt RA, Likhterov I, Scicchitano DA, Geacintov NE, Broyde S. The spacious active site of a Y-family DNA polymerase facilitates promiscuous nucleotide incorporation opposite a bulky carcinogen–DNA adduct: Elucidating the structure–function relationship through experimental and computational approaches. J Biol Chem. 2004; 279:36951–36961. [PubMed: 15210693]
34. Shibutani S, Fernandes A, Suzuki N, Zhou L, Johnson F, Grollman AP. Mutagenesis of the *N*-(deoxyguanosin-8-yl)-2-amino-1-methyl-6-phenylimidazo[4,5-*b*]pyridine DNA adduct in mammalian cells. Sequence context effects. J Biol Chem. 1999; 274:27433–27438. [PubMed: 10488075]
35. Shibutani S, Fernandes A, Suzuki N, Zhou L, Johnson F, Grollman A. Site-specific mutagenesis of the *N*-(deoxyguanosin-8-yl)-2-amino-1-methyl-6-phenylimidazo[4,5-*b*]pyridine DNA adduct in mammalian cells. Z Lebensm-Unters-Forsch. 1998; 207:459–463.
36. Patel DJ, Mao B, Gu Z, Hingerty BE, Gorin A, Basu AK, Broyde S. Nuclear magnetic resonance solution structures of covalent aromatic amine-DNA adducts and their mutagenic relevance. Chem Res Toxicol. 1998; 11:391–407. [PubMed: 9585469]
37. Shibutani S, Grollman AP. Nucleotide misincorporation on DNA templates containing *N*-(deoxyguanosin-N^2-yl-2-(acetylamino)fluorene. Chem Res Toxicol. 1993; 6:819–824. [PubMed: 8117921]
38. Yasui M, Dong H, Bonala RR, Suzuki N, Ohmori H, Hanaoka F, Johnson F, Grollman AP, Shibutani S. Mutagenic properties of 3-(deoxyguanosin-N^2-yl)-2-acetylaminofluorene, a persistent acetylaminofluorene-derived DNA adduct in mammalian cells. Biochemistry. 2004; 43:15005–15013. [PubMed: 15554708]
39. Zaliznyak T, Bonala RR, Johnson F, de los Santos C. Structure and stability of duplex DNA containing the 3-(deoxyguanosin-N^2-yl)-2-acetylaminofluorene (dG(N^2)-AAF) lesion: A bulky adduct that persists in cellular DNA. Chem Res Toxicol. 2006; 19:745–752. [PubMed: 16780352]
40. Koffel-Schwartz N, Verdier JM, Bichara M, Freund AM, Daune MP, Fuchs RP. Carcinogen-induced mutation spectrum in wild-type, uvrA, and umuC strains of *Escherichia coli* Strain specificity and mutation-prone sequences. J Mol Biol. 1984; 177:33–51. [PubMed: 6379196]
41. Doisy R, Tang MS. Effect of aminofluorene and (acetylamino)fluorine adducts on the DNA replication mediated by *Escherichia coli* polymerases I (Klenow fragment) and III. Biochemistry. 1995; 34:4358–4368. [PubMed: 7703249]
42. Koffel-Schwartz N, Coin F, Veaute X, Fuchs RPP. Cellular strategies for accommodating replication-hindering adducts in DNA: Control by the SOS response in *Escherichia coli*. Proc Natl Acad Sci USA. 1996; 93:7805–7810. [PubMed: 8755557]
43. Napolitano RL, Lambert IB, Fuchs RPP. DNA sequence determinants of carcinogen-induced frameshift mutagenesis. Biochemistry. 1994; 33:1311–1315. [PubMed: 8312248]
44. Koffel-Schwartz N, Fuchs RP. Sequence determinants for −2 frameshift mutagenesis at *Nar*I-derived hot spots. J Mol Biol. 1995; 252:507–513. [PubMed: 7563069]

45. Thomas DC, Veaute X, Kunkel TA, Fuchs RP. Mutagenic replication in human cell extracts of DNA containing site-specific *N*-2-acetylaminofluorene adducts. Proc Natl Acad Sci USA. 1994; 91:7752–7756. [PubMed: 8052656]
46. Tan X, Bonala RR, Suzuki N, Johnson F, Grollman AP, Shibutani S. Mutagenic specificity of 2-acetylaminonaphthalene-derived DNA-adduct in mammalian cells. Chem Biol Interact. 2005; 152:131–138. [PubMed: 15840386]
47. Koehl P, Valladier P, Lefevre JF, Fuchs RPP. Strong structural effect of the position of a single acetylaminofluorene within a mutation hot spot. Nucleic Acids Res. 1989; 17:9531–9541. [PubMed: 2602135]
48. Beland FA, Melchior WB, Mourato LLG, Santos MA, Marques MM. Arylamine-DNA adduct conformation in relation to mutagenesis. Mutat Res. 1997; 376:13–19. [PubMed: 9202733]
49. O'Handley SF, Sanford DG, Xu R, Lester CC, Hingerty BE, Broyde S, Krugh TR. Structural characterization of an *N*-acetyl-2-aminofluorene (AAF) modified DNA oligomer by NMR, energy minimization, and molecular dynamics. Biochemistry. 1993; 32:2481–2497. [PubMed: 8448107]
50. Gu Z, Gorin A, Krishnasamy R, Hingerty BE, Basu AK, Broyde S, Patel DJ. Solution structure of the *N*-(deoxyguanosin-8-yl)-1-aminopyrene ([AP]dG) adduct opposite dA in a DNA duplex. Biochemistry. 1999; 38:10843–10854. [PubMed: 10451381]
51. Gu Z, Gorin A, Hingerty BE, Broyde S, Patel DJ. Solution structures of aminofluorene [AF]-stacked conformers of the *syn* [AF]-C8-dG adduct positioned opposite dC or dA at a template–primer junction. Biochemistry. 1999; 38:10855–10870. [PubMed: 10451382]
52. Mao B, Gorin A, Gu Z, Hingerty BE, Broyde S, Patel DJ. Solution structure of the aminofluorene-intercalated conformer of the *syn* [AF]-C8-dG adduct opposite a −2 deletion site in the *NarI* hot spot sequence context. Biochemistry. 1997; 36:14479–14490. [PubMed: 9398167]
53. Mao B, Gu Z, Gorin A, Hingerty BE, Broyde S, Patel DJ. Solution structure of the aminofluorene-stacked conformer of the *syn* [AF]-C8-dG adduct positioned at a template–primer junction. Biochemistry. 1997; 36:14491–14501. [PubMed: 9398168]
54. Mao B, Hingerty BE, Broyde S, Patel DJ. Solution structure of the aminofluorene [AF]-intercalated conformer of the *syn*-[AF]-C8-dG adduct opposite dC in a DNA duplex. Biochemistry. 1998; 37:81–94. [PubMed: 9425028]
55. Mao B, Hingerty BE, Broyde S, Patel DJ. Solution atructure of the aminofluorene [AF]-external conformer of the *anti*-[AF]-C8-dG adduct opposite dC in a DNA duplex. Biochemistry. 1998; 37:95–106. [PubMed: 9425029]
56. Zhou L, Rajabzadeh M, Traficante D, Cho BP. Conformational heterogeneity of arylamine-modified DNA: ^{19}F NMR evidence. J Am Chem Soc. 1997; 119:5384–5389.
57. Cho BP, Beland FA, Marques MM. NMR structural studies of a 15-mer DNA duplex from a rat protooncogene modified with the carcinogen 2-aminofluorene: Conformational heterogeneity. Biochemistry. 1994; 33:1373–1384. [PubMed: 8312255]
58. Cho BP, Zhou L. Probing the conformational heterogeneity of the acetylaminofluorene-modified 2′-deoxyguanosine and DNA by ^{19}F NMR spectroscopy. Biochemistry. 1999; 38:7572–7583. [PubMed: 10360955]
59. Cho BP, Beland FA, Marques MM. NMR structural studies of a 15-mer DNA sequence from a *ras* protooncogene, modified at the first base of codon 61 with the carcinogen 4-aminobiphenyl. Biochemistry. 1992; 31:9587–9602. [PubMed: 1327120]
60. Milhe C, Fuchs RPP, Lefevre JF. NMR data show that the carcinogen *N*-2-acetylaminoflurorene stabilizes an intermediate of −2 frameshift mutagenesis in a region of high mutation frequency. Eur J Biochem. 1996; 235:120–127. [PubMed: 8631318]
61. Milhe C, Dhalluin C, Fuchs RPP, Lefevre JF. NMR evidence of the stabilization by the carcinogen *N*-2-acetylaminoluorene of a frameshift mutagenesis intermediate. Nucleic Acids Res. 1994; 22:4646–4652. [PubMed: 7984413]
62. Abuaf P, Hingerty BE, Broyde S, Grunberger D. Solution conformation of the *N*-(deoxyguanosin-8-yl)aminofluorene adduct opposite deoxyinosine and deoxyguanosine in DNA by NMR and computational characterization. Chem Res Toxicol. 1995; 8:369–378. [PubMed: 7578923]

63. Brown K, Hingerty BE, Guenther EA, Krishnan VV, Broyde S, Turteltaub KW, Cosman M. Solution structure of the 2-amino-1-methyl-6-phenylimidazo[4,5-*b*]pyridine C8-deoxyguanosine-adduct in duplex DNA. Proc Natl Acad Sci USA. 2001; 98:8507–8512. [PubMed: 11438709]
64. Dutta S, Li Y, Johnson D, Dzantiev L, Richardson CC, Romano LJ, Ellenberger T. Crystal structures of 2-acetylaminofluorene and 2-aminofluorene in complex with T7 DNA polymerase reveal mechanisms of mutagenesis. Proc Nat Acad Sci USA. 2004; 101:16186–16191. [PubMed: 15528277]
65. Hsu GW, Kiefer JR, Burnouf D, Becherel OJ, Fuchs RPP, Beese LS. Observing translesion synthesis of an aromatic amine DNA adduct by a high-fidelity DNA polymerase. J Biol Chem. 2004; 279:50280–50285. [PubMed: 15385534]
66. Maenhaut-Michel G, Janel-Bintz R, Samuel N, Fuchs RPP. Adducts formed by the food-mutagen 2-amino-3-methylimidazo[4,5-*f*]quinoline (IQ) induce frameshift mutations at hotspots through an SOS-independent pathway. Mol Gen Genet. 1997; 253:634–641. [PubMed: 9065697]
67. Solomon MS, Morgenthaler PML, Turesky RJ, Essigmann JM. Mutational and DNA binding specificity of the carcinogen 2-amino-3,8-dimethylimidazo[4,5-*f*]quinoxaline. J Biol Chem. 1996; 271:18368–18374. [PubMed: 8702479]
68. Lindsley JE, Fuchs RPP. Use of single-turnover kinetics to study bulky adduct bypass by T7 DNA polymerase. Biochemistry. 1994; 33:764–772. [PubMed: 8292604]
69. Dzantiev L, Romano LJ. Interaction of *Escherichia coli* DNA polymerase I (Klenow fragment) with primer–templates containing *N*-acetyl-2-aminofluorene or *N*-2-aminofluorene adducts in the active site. J Biol Chem. 1999; 274:3279–3284. [PubMed: 9920867]
70. Gill JP, Romano LJ. Mechanism for *N*-acetyl-2-aminofluorene-induced frameshift mutagenesis by *Escherichia coli* DNA polymerase I (Klenow fragment). Biochemistry. 2005; 44:15387–15395. [PubMed: 16285743]
71. Napolitano R, Janel-Bintz R, Wagner J, Fuchs RP. All three SOS-inducible DNA polymerases (Pol II, Pol IV, and Pol V) are involved in induced mutagenesis. EMBO J. 2000; 19:6259–6265. [PubMed: 11080171]
72. Fuchs RP, Koffel-Schwartz N, Pelet S, Janel-Bintz R, Napolitano R, Becherel OJ, Broschard TH, Burnouf DY, Wagner J. DNA polymerases II and V mediate respectively mutagenic (−2 frameshift) and error-free bypass of a single *N*-2-acetylaminofluorene adduct. Biochem Soc Trans. 2001; 29:191–195. [PubMed: 11356152]
73. Becherel OJ, Fuchs RPP. Mechanism of DNA polymerase II-mediated frameshift mutagenesis. Proc Natl Acad Sci USA. 2001; 98:8566–8571. [PubMed: 11447256]
74. Choi JY, Stover JS, Angel KC, Chowdhury G, Rizzo CJ, Guengerich FP. Biochemical basis of genotoxicity of heterocyclic arylamine food mutagens: Human DNA polymerase η selectively produces a two-base deletion in copying the N2-guanyl-adduct of 2-amino-3-methylimidazo[4,5-*f*]quinoline but not the C8-adduct at the *Nar*I G3 site. J Biol Chem. 2006; 281:25297–25306. [PubMed: 16835218]
75. Boudsocq F, Iwai S, Hanaoka F, Woodgate R. *Sulfolobus solfataricus* P2 DNA polymerase IV (Dpo4): An archaeal DinB-like DNA polymerase with lesion-bypass properties akin to eukaryotic polη. Nucleic Acids Res. 2001; 29:4607–4616. [PubMed: 11713310]
76. Fuchs RP, Fujii S, Wagner J. Properties and functions of *Escherichia coli*: Pol IV and Pol V. Adv Protein Chem. 2004; 69:229–264. [PubMed: 15588845]
77. Ling H, Sayer JM, Plosky BS, Yagi H, Boudsocq F, Woodgate R, Jerina DM, Yang W. Crystal structure of a benzo[*a*]pyrene diol epoxide adduct in a ternary complex with a DNA polymerase. Proc Natl Acad Sci USA. 2004; 101:2265–2269. [PubMed: 14982998]
78. Ling H, Boudsocq F, Woodgate R, Yang W. Snapshots of replication through a basic lesion: Structural basis for base substitutions and frameshifts. Mol Cell. 2004; 13:751–762. [PubMed: 15023344]
79. Ling H, Boudsocq F, Woodgate R, Yang W. Crystal structure of a Y-family DNA polymerase in action: a mechanism for error-prone and lesion-bypass replication. Cell. 2001; 107:91–102. [PubMed: 11595188]
80. Ling H, Boudsocq F, Plosky BS, Woodgate R, Yang W. Replication of a *cis–syn* thymine dimer at atomic resolution. Nature. 2003; 424:1083–1087. [PubMed: 12904819]

81. Suzuki N, Ohashi E, Hayashi K, Ohmori H, Grollman AP, Shibutani S. Translesional synthesis past acetylaminofluorene-derived DNA adducts catalyzed by human DNA polymerase κ and *Escherichia coli* DNA polymerase IV. Biochemistry. 2001; 40:15176–15183. [PubMed: 11735400]
82. Wang L, Broyde S. A new anti conformation for *N*-(deoxyguanosin-8-yl)-2-acetylaminofluorene (AAF-dG) allows Watson–Crick pairing in the *Sulfolobus solfataricus* P2 DNA polymerase IV (Dpo4). Nucleic Acids Res. 2006; 34:785–795. [PubMed: 16452300]
83. Shibutani S, Suzuki N, Grollman AP. Mechanism of frameshift (deletion) generated by acetylaminofluorene-derived DNA adducts in vitro. Biochemistry. 2004; 43:15929–15935. [PubMed: 15595849]
84. Nair DT, Johnson RE, Prakash L, Prakash S, Aggarwal AK. Human DNA polymerase ι incorporates dCTP opposite template G via a G·C+ Hoogsteen base pair. Structure. 2005; 13:1569–1577. [PubMed: 16216587]
85. Nair DT, Johnson RE, Prakash S, Prakash L, Aggarwal AK. Replication by human DNA polymerase ι occurs by Hoogsteen base pairing. Nature. 2004; 430:377–340. [PubMed: 15254543]
86. Johnson RE, Prakash L, Prakash S. Biochemical evidence for the requirement of Hoogsteen base pairing for replication by human DNA polymerase ι. Proc Natl Acad Sci USA. 2005; 102:10466–10471. [PubMed: 16014707]
87. Broschard TH, Lebrun-Garcia A, Fuchs RP. Mutagenic specificity of the food mutagen 2-amino-3-methylimidazo-[4,5-*f*]quinoline in *Escherichia coli* using the yeast URA3 gene as a target. Carcinogenesis. 1998; 19:305–310. [PubMed: 9498281]
88. Pham P, Rangarajan S, Woodgate R, Goodman MF. Roles of DNA polymerases V and II in SOS-induced error-prone and error-free repair in *Escherichia coli*. Proc Natl Acad Sci USA. 2001; 98:8350–8354. [PubMed: 11459974]
89. Qiu Z, Goodman MF. The *Escherichia coli polB* locus is identical to *dinA*, the structural gene for DNA polymerase II. Characterization of Pol II purified from a *polB* mutant. J Biol Chem. 1997; 272:8611–8617. [PubMed: 9079692]

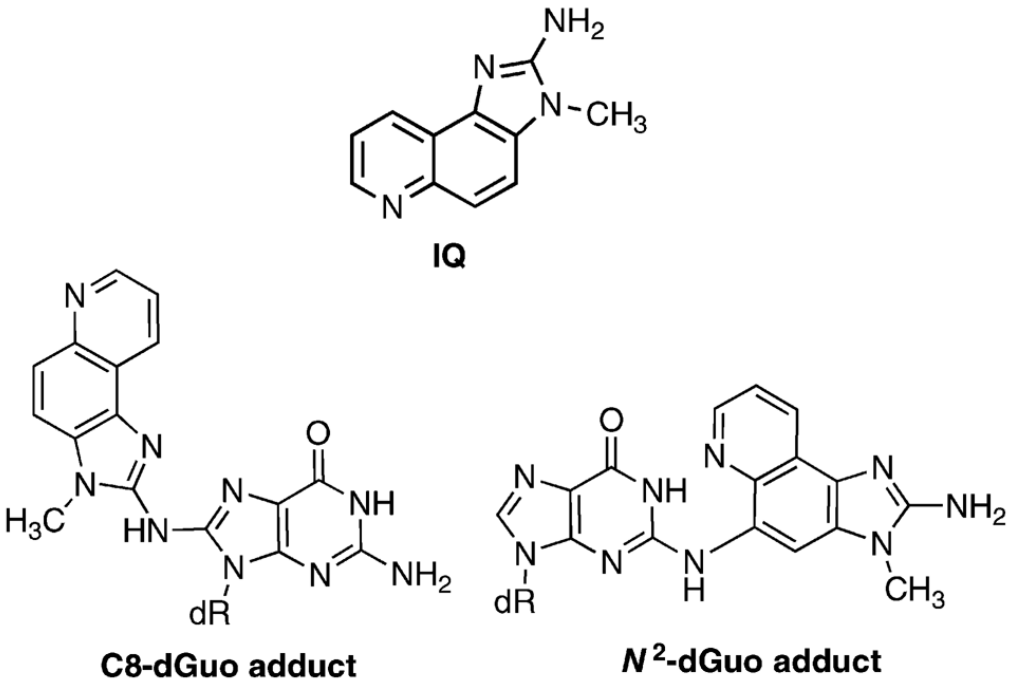

Figure 1.
Structures of IQ and its C8- and N^2-dGuo-adducts.

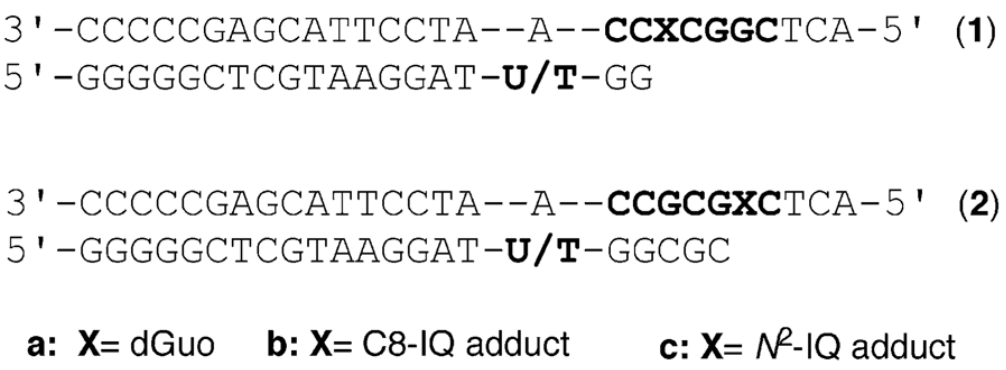

Figure 2.
Modified oligonucleotides (**1** and **2**) and primers used in extension reactions.

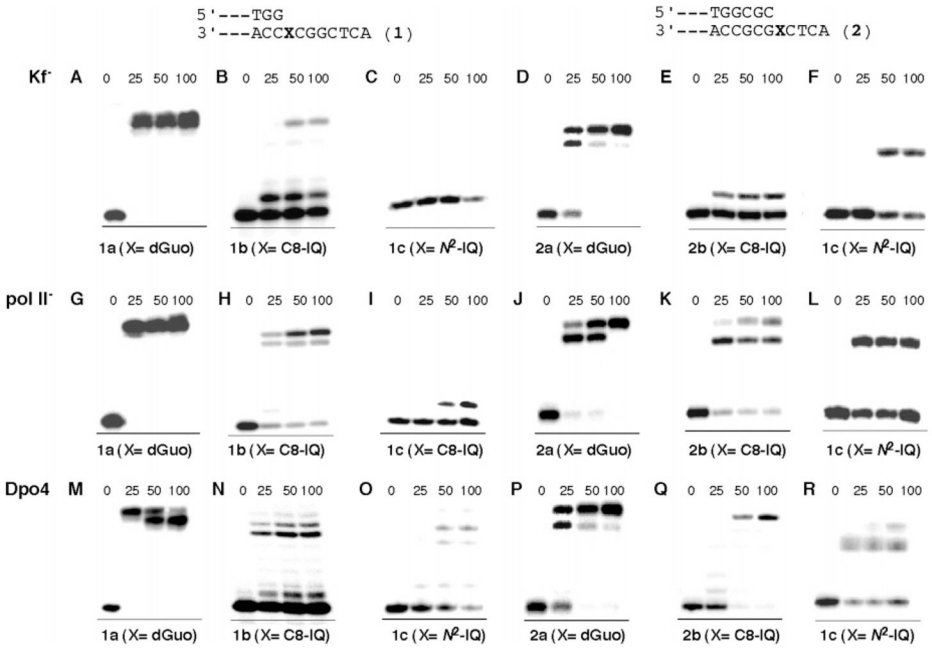

Figure 3.
Full-length extension of the oligonucleotides **1** and **2** by Kf^{-}, pol II^{-}, and Dpo4.

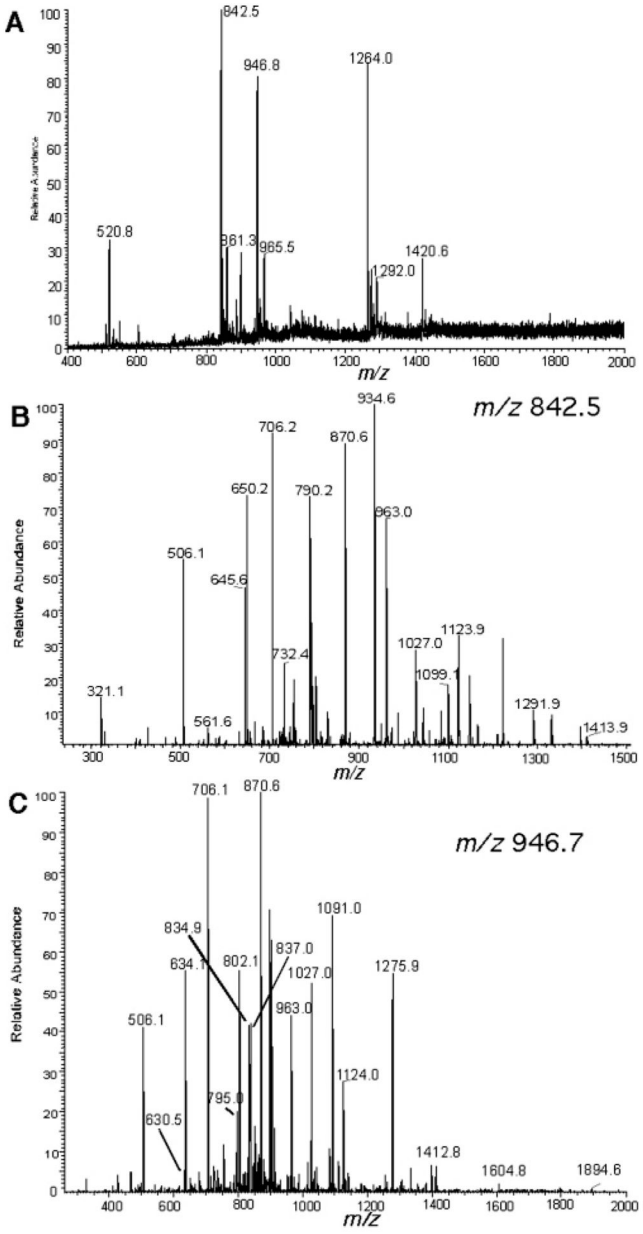

Figure 4.

LC-MS/MS analysis of the Kf⁻ extension products of oligonucleotide **1b**. (A) TIC spectrum; (B) CID spectrum from *m*/*z* 946.7; and (C) CID spectrum from *m*/*z* 842.5.

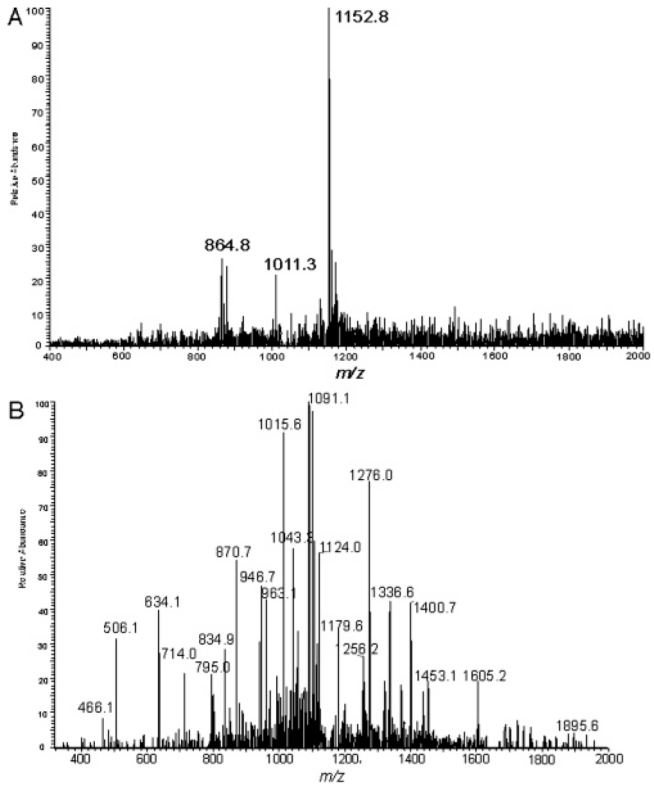

Figure 5.
LC-MS/MS analysis of the Kf^{-} extension products of oligonucleotide **2c**. (A) TIC spectrum and (B) CID spectrum of *m*/*z* 1152.8.

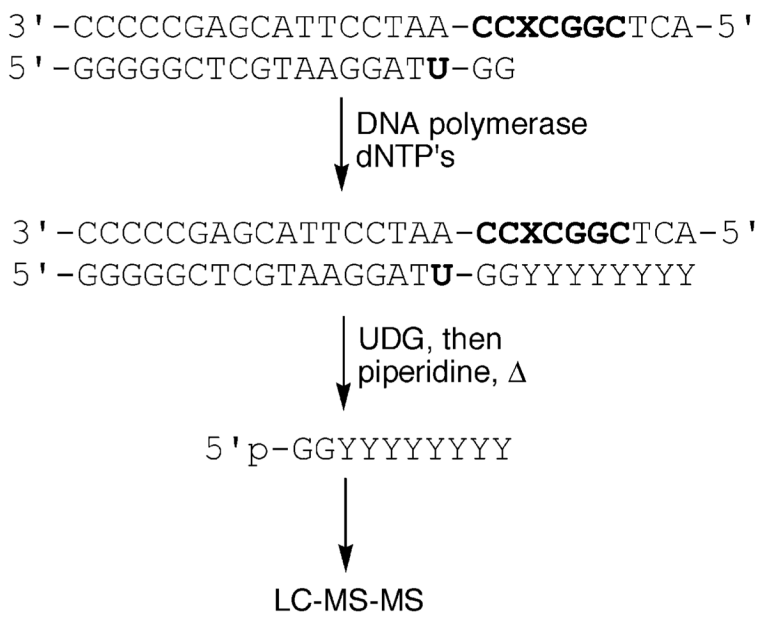

Scheme 1.
LC-MS/MS Sequencing

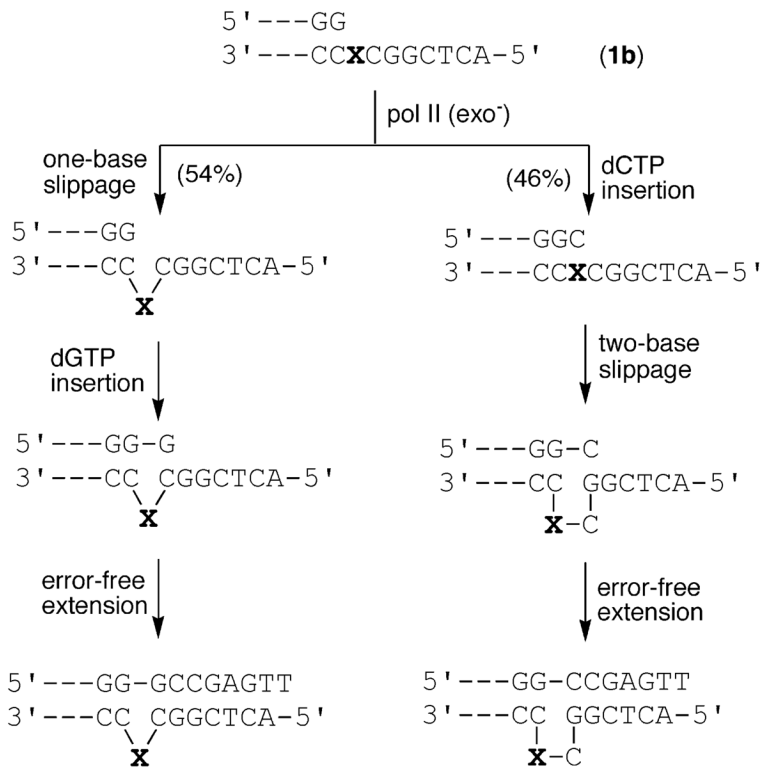

Scheme 2.

One- and Two-Base Slippage Mechanism for pol II^{-} Bypass of the C8-IQ-Adduct in the Dinucleotide Repeat Position of the *Nar*I Sequence (1b)

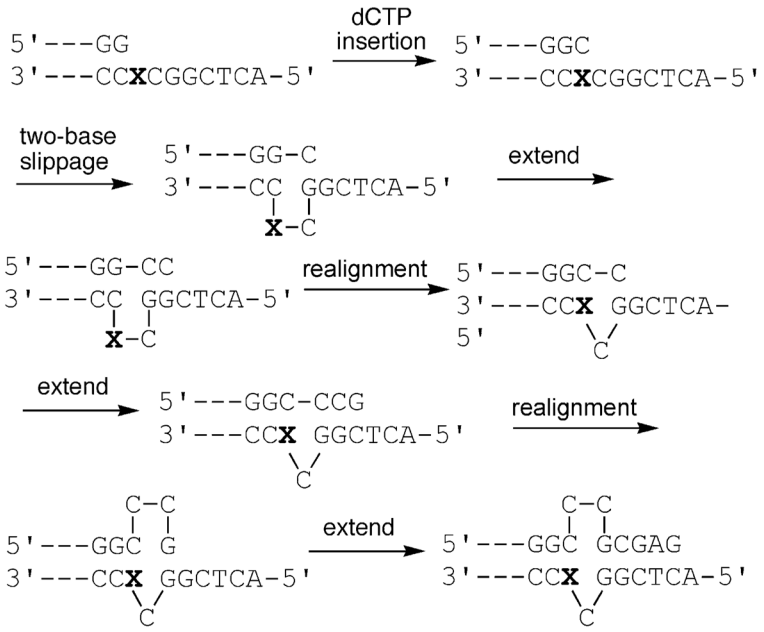

Scheme 3.
Mechanism for the Bypass and Extension of Modified Template 1b by Dpo4

Table 1

Steady-State Kinetic Parameters for Single-Nucleotide Incorporation Opposite the C8- and N^2-IQ-Adducts at the G_3- and G_1-Positions of the *Nar*I Recognition Sequence by Kf^-

template	X	dNTP	k_{cat} ($s^{-1} \times 10^{-3}$)	K_m (μM)	k_{cat}/K_m ($\mu M^{-1}\ s^{-1} \times 10^{-3}$)
1	**a** (dGuo)	C	46 ± 5.5	0.29 ± 0.05	160
	b (C8)	C	1.3 ± 0.04	19 ± 5	0.068
	c (N^2)	C	<0.1	>500	
2	**a** (dGuo)	C	65 ± 9	0.18 ± 0.03	360
	b (C8)	C	0.66 ± 0.02	52 ± 9.3	0.013
	c (N^2)	C	0.32 ± 0.05	38 ± 6.6	0.008

Table 2

Observed and Theoretical Fragmentation for the Kf⁻ Extension Products of 1b

A. 5′-pGGCCGAGT-3′, *m/z* 842.5 (M-3H)		
Fragment assignment	**observed**	**theoretical**
5′-pG (a_2-B)	506.1	506.05
5′-pGGC (a_4-B)	1123.9	1124.68
(a_4-B, −2)	561.6	561.84
5′-pGGCC (a_5-B)	1413.9	1413.87
(a_5-B, −2)	706.2	706.43
5′-pGGGCC (a_6-B, −2)	870.6	871.03
5-pGGGCCG (a_7-B, −2)	1027.0	1027.64
pGCCGAGT-3′ (w_7, −2)	1099.1	1099.70
pCCGAGT-3′ (w_6, −2)	934.6	935.10
pCGAGT-3′ (w_5, −2)	790.2	790.51
pGAGT-3′ (w_4)	1291.9	1292.83
(w_4, −2)	645.6	645.91
pAGT-3′ (w_3)	963.0	963.62
pGT-3′ (w_2)	650.2	650.41
p-T-3′ (w_1)	321.1	321.20

B. 5′-pGGCCGAGTA-3′, *m/z* 946 (M-3H)		
Fragment assignment	**observed**	**theoretical**
5′-pG (a_2-B)	506.1	506.05
5′-pGG (a_3-B)	834.9	835.10
5′-pGGC (a_4-B)	1124.0	1124.14
5′-pGGCC (a_5-B)	1412.8	1413.19
(a_5-B, −2)	706.1	706.09
5′-pGGCCG (a_6-B, −2)	870.6	870.62
5-pGGCCGA (a_7-B, −2)	1027.0	1027.15
pCCGAGTA-3′ (w_7)	1091.0	1091.18
pGAGTA-3′ (w_5)	1604.8	1605.27
(w_5, −2)	802.1	802.13
pAGTA-3′ (w_4)	1275.9	1276.21
pGTA-3′ (w_3)	963.0	963.16
p-TA-3′ (w_2)	634.1	634.11

Table 3

Observed and Theoretical Fragmentation for the Kf^{-} Extension Products of Oligonucleotide 2c

5′-pGGCGCCGAGTA-3′, m/z 1152.8 (M-3H)

Fragment assignment	observed mass	theoretical mass
5′-pG (a_2-B)	506.1	506.05
5′-pGG (a_3-B)	834.1	835.1
5′-pGGC (a_4-B)	1124.0	1124.68
5′-pGGCG (a_5-B)	1452.1	1453.20
5′-pGGCGC (a_6-B, −2)	870.7	870.62
5-pGGCGCC (a_7-B, −2)	1015.6	1015.14
5-pGGCGCCG (a_8-B, −2)	1179.6	1179.67
5-pGGCGCCGA (a_9-B, −2)	1336.06	1336.20
pGCGCCGAGTA-3′ (w_9, −2)	1400.7	1400.22
pCGCCGAGTA-3′ (w_8, −2)	1256.2	1255.70
pGCCGAGTA-3′ (w_7, −2)	1091.1	1091.18
pCCGAGTA-3′ (w_6)	1895.6	1894.31
pCGAGTA-3′ (w_6, −2)	946.7	946.65
pGAGTA-3′ (w_5)	1605.2	1605.27
pAGTA-3′ (w_4)	1276.0	1276.21
pGTA-3′ (w_3)	963.1	963.16
p-TA-3′ (w_2)	634.1	634.11

Table 4

Summary of the Kf⁻ Extension of IQ-dGuo-Modified Oligonucleotides.

template		extension products identified by MS	comments
3′----**CC<u>X</u>CGGC**TCA-5′	**<u>X</u>** = C8-IQ (**1b**)	5′-pGGCCGAGT-3′, 5′-pGGCCGAGTA-3′	two-base deletion products
	<u>X</u> = N^2-IQ (**1c**)		insertion inhibited
3′----**CCGCG<u>X</u>C**TCA-5′	**<u>X</u>** = C8-IQ (**2b**)		extension inhibited
	<u>X</u> = N^2-IQ (**1c**)	5′-pGGCGCCGAGTA-3′	error-free product

Table 5

Steady-State Kinetic Parameters for Single-Nucleotide Incorporation Opposite the C8- and N^2-IQ-Adducts at the G_3- and G_1-Positions of the *Nar*I Recognition Sequence by *E. coli* pol II (exo$^-$)

template	X =	dNTP	k_{cat} ($s^{-1} \times 10^{-3}$)	K_m (μM)	k_{cat}/K_m ($\mu M^{-1}\ s^{-1} \times 10^{-3}$)	f^a
1	**a** (dGuo)	C	15 ± 1	0.25 ± 0.05	60	1
		G	0.46 ± 0.02	5 ± 1	0.092	0.002
	b (C8)	C	0.32 ± 0.03	240 ± 30	0.001	1
		G	1.7 ± 0.13	40 ± 10	0.043	43
	c (N^2)	C	0.28 ± 0.01	64 ± 11	0.004	1
		G	0.19 ± 0.01	110 ± 16	0.002	0.5
2	**a** (dGuo)	C	21 ± 2	0.36 ± 0.02	58	1
	b (C8)	C	0.44 ± 0.03	20 ± 7	0.022	1
	c (N^2)	C	0.21 ± 0.02	26 ± 7	0.008	1

[a] f = misincorporation frequency = $(k_{cat}/K_m)_{incorrect\ dNTP}/(k_{cat}/K_m)_{correct\ dNTP\ (dCTP)}$.

Table 6

Summary of the pol II⁻ Extension of IQ-dGuo-Modified Oligonucleotides

template		extension products identified by MS	comments
3′----**CCXCGGC**TCA-5′	**X** = C8-IQ (**1b**)	5′-pGGCCGAGTT, 5′-pGGGCCGAGTT-3′	two- and one-base deletion products
	X = N^2-IQ (**1c**)		extension inhibited
3′----**CCGCGXC**TCA-5′	**X** = C8-IQ (**2b**)	5′-pGGCGCCGAGTA-3′	error-free product
	X = N^2-IQ (**1c**)	5′-pGGCGCCGAGT-3′	error-free product

Table 7

Steady-State Kinetic Parameters for Single-Nucleotide Incorporation Opposite the C8- and N^2-IQ-Adducts at the G_3- and G_1-Positions of the *Nar*I Recognition Sequence by Dpo4

template	X	dNTP	k_{cat} ($s^{-1} \times 10^{-3}$)	K_m (μM)	k_{cat}/K_m ($\mu M^{-1}\ s^{-1} \times 10^{-3}$)	f^a
1	**a** (dGuo)	C	2.23 ± 0.4	0.13 ± 0.02	17.2	1
		T	0.55 ± 0.02	14 ± 2	0.04	0.002
	b (C8)	C	0.44 ± 0.02	11 ± 2	0.040	1
		T	0.34 ± 0.03	66 ± 2	0.005	0.13
	c (N^2)	C	0.29 ± 0.02	69 ± 4	0.004	1
		T	0.23 ± 0.01	84 ± 8	0.003	0.75
2	**a** (dG)	C	1.8 ± 0.5	0.21 ± 0.05	8.6	1
		T	0.25 ± 0.01	85 ± 8	0.003	0.0004
		A	0.18 ± 0.01	114 ± 13	0.002	0.0002
		G	0.21 ± 0.02	96 ± 9	0.002	0.0002
	b (C8)	C	0.42 ± 0.03	22 ± 4	0.019	1
	c (N^2)	C	0.22 ± 0.02	20 ± 2	0.011	1
		T	0.18 ± 0.05	36 ± 3	0.005	0.46
		A	0.11 ± 0.04	120 ± 22	0.001	0.091
		G	0.14 ± 0.05	82 ± 7	0.002	0.18

[a] f = misincorporation frequency = $(k_{cat}/K_m)_{incorrect\ dNTP}/(k_{cat}/K_m)_{correct\ dNTP\ (dCTP)}$.

Table 8

Summary of the Dpo4 Extension of IQ-dGuo-Modified Oligonucleotides

template		extension products identified by MS	comments
3′----**CCXCGGC**TCA-5′	**X** = C8-IQ (**1b**)	5′-pGGCCCGCGAG-3′	two-base deletion and error prone extension
	X = N^2-IQ (**1c**)	5′-pGGCGCCGAGTA-3′	error-free product
3′----**CCGCGXC**TCA-5′	**X** = C8-IQ (**2b**)	5′-pGGCGCCGAGT-3′	error-free product
	X = N^2-IQ (**1c**)	5′-pGGCGCCGAGT-3′	error-free product